Supporting Information For:

Ice multiplication from ice-ice collisions in the high Arctic: sensitivity to ice habit, rimed fraction and the spectral representation of the colliding particles

Georgia Sotiropoulou[1,2], Luisa Ickes[3], Athanasios Nenes[2,4] and Annica M. L. Ekman[1]

[1]Department of Meteorology, Stockholm University & Bolin Center for Climate Research, Stockholm, Sweden
[2]Laboratory of Atmospheric Processes and their Impacts, School of Architecture, Civil & Environmental Engineering, Ecole Polytechnique Fédérale de Lausanne, Lausanne, Switzerland
[3]Department of Space, Earth and Environment, Chalmers University of Technology, Gothenburg, Sweden
[4]Institue for Chemical Engineering Sciences, Foundation for Research and Technology Hellas, Patras, Greece

Correspondence to: georgia.sotiropoulou@misu.su.se

This PDF file includes:

Supplementary Text S1 to S2

Supplementary Figures S1 to S4

Text S1: Constraining Primary Ice Nucleation in MIMICA

In the empirical ice nucleation active site density parameterization for immersion freezing, implemented in MIMICA by Ickes et al. (2020), it is assumed that a specified fraction of the CCN population contains microline, an efficient ice-nucleating feldspar type (see Section 3.2.1 in the main text for a discussion). The sensitivity of the calculated INP to the number of CCN and the percentage of microline is investigated in Ickes et al. (2020) using the same ASCOS case study. Here we use 50% microline, 10% microline (also tested in their study) and further test an even lower value by assuming that only 5% of N_{CCN} act as INPs (Fig. S1); this simulation is referred as 5% microline in this text.

The 50% microline results in improved representation of the available liquid (LWP) and ice (IWP) water path during the first 12 hours compared to the observations, but eventually the cloud glaciates at the end of the simulation (Fig. S1a,b). LWP and IWP are more similar between 5% and 10% microline, with the latter producing somewhat larger (smaller) IWP (LWP). Droplet concentrations are also more similar in these two simulations (Figure S1c), while distinct differences are found in ICNCs (Fig. S1d). Maximum ICNC increases as minimum mean in-cloud temperature decreases from -10.4^{o}C, after spin-up, to -12.4^{o}C at the end of the simulation (not shown), owing to cloud-top radiative cooling. Within this period, the corresponding maximum total ICNC increases from 0.8 to 2.7 L^{-1} in 10% microline and from 0.3 to 1 L^{-1} in 5% microline. Total ICNCs in all simulations consist mainly of graupel, along with low concentrations of cloud ice; no snow is produced in any simulation (Fig. S1d). In 50% microline total ICNCs increase from 4 L^{-1} to 12.2 L^{-1} at hour 19, after which the cloud begins gradually dissipating. This behavior is in agreement with Lowe et al. (2018), whom also showed that ICNCs exceeding 10 L^{-1} result in cloud glaciation.

Wex et al. (2019) recently presented a synthesis of long-term INP measurements from several Arctic sites and published literature; all these measurements indicate that INPs do not exceed 0.2-0.7 L^{-1} at temperatures between -10^{o}C and -12.5^{o}C (see Figure 7 in Wex et al 2019). These results indicate that assuming 10% and especially 50% microline overpredict INP concentrations (Fig. 4a,b). For this reason, we adapt the 5% microline freezing parameterization, which underestimates (overestimates) IWP (LWP), but produces more realistic primary ICNCs (Fig. S1d). While primary ice nucleation is still likely overestimated in our simulations, this approach ensures that underestimates in cloud ice content are not due to underprediction of the INPs.

Text S2: ICNC enhancement in simulations with active collisional break-up

ICNC enhancement due to break-up is calculated in this section by dividing the total ICNCs produced in each simulation with active ice multiplication with those produced by the control simulation that accounts only for primary ice. In simulations with dendrites, for primary ICNCs larger than 0.05 L^{-1}, ICNC enhancement rarely exceeds a factor of 2 in BRDEN0.2 simulation (Fig. S2a). Somewhat larger enhancements can be found in BRDEN0.3 and BRDEN0.4, reaching up to a factor of 3-4 (Figure S2b-c). In all three panels the larger fluctutations correpond to primary ICNCs < 0.05 L^{-1}.

In simulation with plates (Fig. S3), variations of Ψ in the break-up parameterization lead to very different resuts. The ICNC enhancement factor in BRPLA0.2 remains usually below 2 (Figure S3d), while greater enhancements are only observed when primary ICNCs are between 0.2-0.4 L^{-1}. Increasing Ψ to 0.3 and 0.4 results in maximum ICNC enhancements of the order of 80 and 900; such large enhancements lead to cloud glaciation and are rather unrealistic for the examined case study.

Activating cloud ice-to-snow autoconversion, with the separation diameter set to 125 μm, results in enhanced primary ICNCs in both CNTRLDENauto1 and CNTRPLAauto1 simulations. Maximum ICNCs reach up to 2 L^{-1} (Fig. S3), which is about two times larger than maximum values in CNTRLDEN and CNTRLPLA, respectively (Fig. S2). This is due to the fact that increasing snow formation is accompanied by decreasing graupel concentration in these simulations (see Section 4.3.1 for a discussion), which enentually results in less ice precipitation. Nevertheless the enhanced ICNCs due to active autoconversion can still not reproduce the observed cloud water properties (Figs. 6-8 in main text).

Activating break-up for this setting, while assuming a dendritic ice habit and that Ψ=0.2 (Fig. S3a), results in weak ICNC enhancement rarely exceeding a factor of 2, when primary ICNCs are > 0.1 L^{-1}; when Ψ=0.4 (Fig. S3b) the enhancement generelly shifts to larger values, between a factor of 2-3. Break-up of lightly rimed planar ice results in weaker enhancements, hardly ever exceeding a factor of 1.5 (Fig. S3c), while break-up of highly rimed plates can enhance primary ICNCs by up to a factor of 3-4. The largest ICNC enhancements correspond to very low primary ICNC concentrations < 0.1 L^{-1} in all simulations, which can sometimes exceed a factor of 10.

Increasing the critical diameter that determines cloud ice-to-snow autoconversion results in fewer primary ICNCs in CNTRLDENauto2/ CNTRLPLAauto2 (Fig. S4) compared to CNTRLDENauto1/ CNTRLPLAauto2 (Fig S3). However for a given primary ICNC range, the enhancements due to break-up are either similar or weaker with increasing separation diameter. (Fig. S4).

Figures:

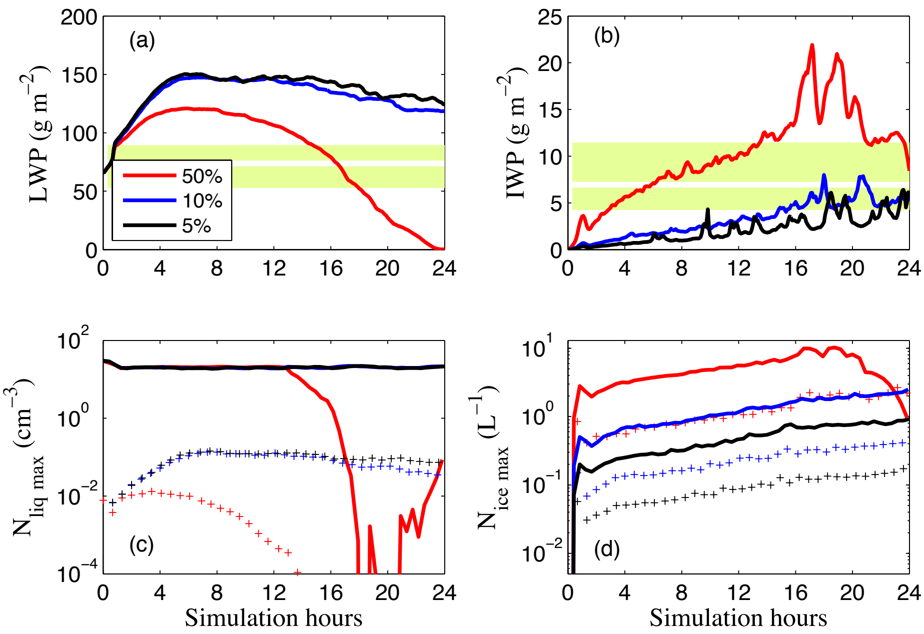

Figure S1: Timeseries of domain-averaged (a) liquid water path (LWP), (b) ice water path (IWP), maximum domain-averaged (c) liquid and (d) ice number concentration for three different immersion freezing settings (see section 3.2.1). Light green shaded area in panels (a) and (b) indicate the interquartile range of observations, while the horizontal white line shows median observed values. Solid lines in panel (c) indicate cloud droplets, while crosses represent raindrops (size > 25 μm). Solid lines in panel (d) indicate graupels, while crosses represent cloud ice; no snow is produced. Secondary ice production is inactive in these simulations. A dendritic ice habit is assumed, which is reasonable for the examined temperature range (Pruppacher and Klett, 1997).

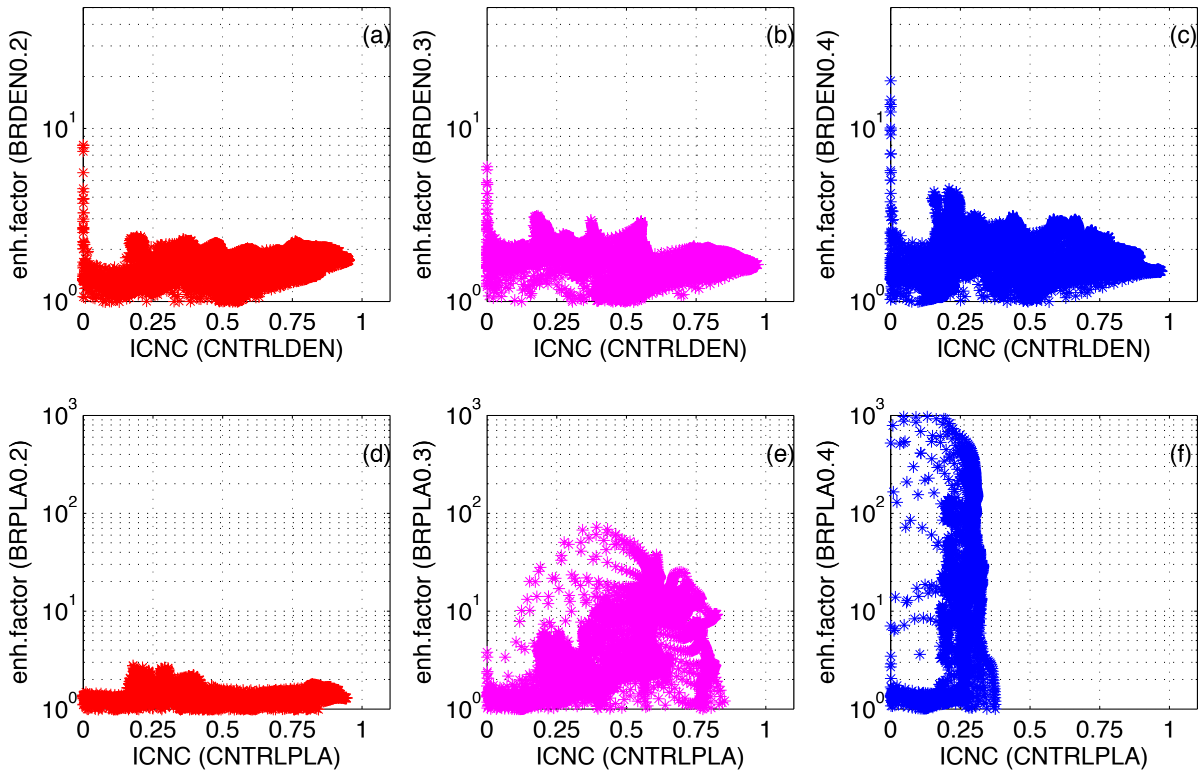

Figure S2: Scatterplots of primary ICNCs (L^{-1}) from the control simulation and the factors in simulations with break-up (see Text S2 for detailed calculations). Panels (a-c) correspond to simulations with a dendritic ice habit, while (d-f) to simulations with planar ice. Results are shown for different assumptions in the rimed fraction (Ψ) of the particles that undergo break-up: (a, d) Ψ=0.2, (b, e) Ψ=0.3, (c, f) Ψ=0.4. In all simulations cloud ice-to-snow autoconversion is inactive (see Table 2 in main text for a summary of the simulation set-ups).

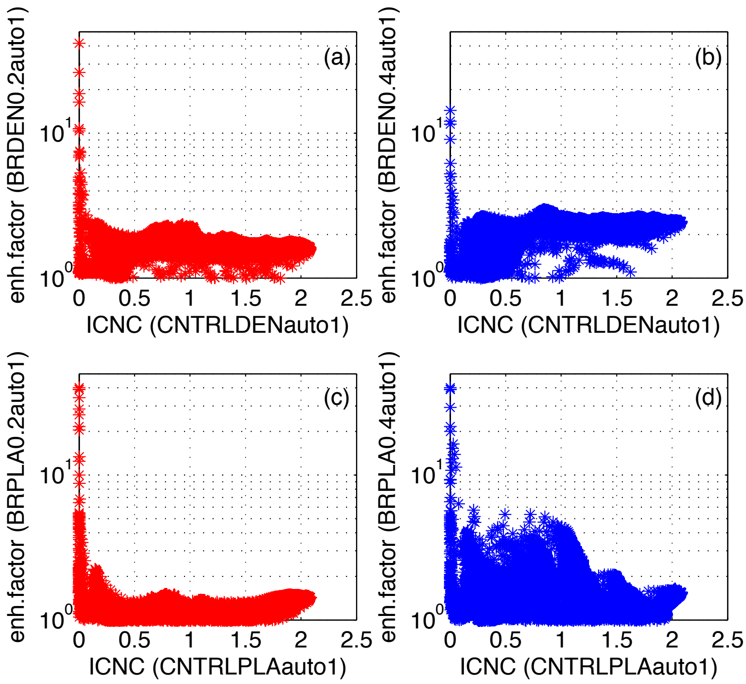

Figure S3: Similar to Fig. S2, but for simulations with active cloud ice-to-snow autoconversion. Panels (a-b) correspond to simulations with a dendritic ice habit, while (c-d) to simulations with planar ice. Results are shown for different assumptions in the rimed fraction (Ψ) of the particles that undergo break-up: (a, c) Ψ=0.2 and (b, d) Ψ=0.4. The separation diameter for the autoconversion process is set to 125 μm (see Table 2 in the main text).

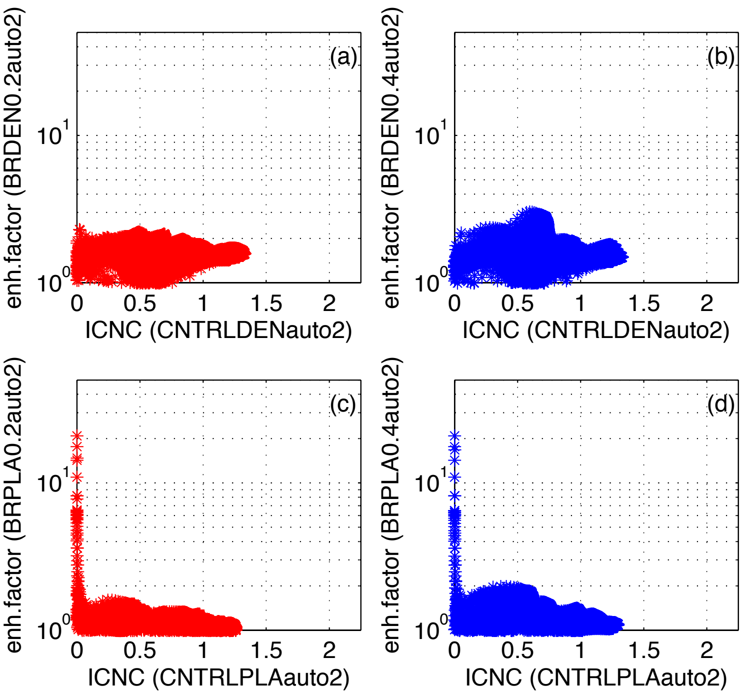

Figure S4: Same as Fig. S3 but with the separation diameter set to 500 µm (see Table 2 in the main text)